

Terahertz emission from GaAs-AlGaAs core-shell nanowires on Si(100) substrate: Effects of applied magnetic field and excitation wavelength

メタデータ	言語: English
	出版者:
	公開日: 2014-01-31
	キーワード (Ja):
	キーワード (En):
	作成者: Ibanes, Jasher John, Balgos, Ma. Herminia, Jaculbia, Rafael, Salvador, Arnel, Somintac, Armando, Estacio, Elmer, Que, Christopher T., Tsuzuki, Satoshi, Yamamoto, Kohji, Tani, Masahiko
	メールアドレス:
URL	所属:
	http://hdl.handle.net/10098/8074

© 2013 AIP Publishing LLC. This article may be downloaded for personal use only. Any other use requires prior permission of the author and the American Institute of Physics.



Terahertz emission from GaAs-AlGaAs core-shell nanowires on Si (100) substrate: Effects of applied magnetic field and excitation wavelength

Jasher John Ibanes,^{1,a)} Ma. Herminia Balgos,¹ Rafael Jaculbia,¹ Arnel Salvador,¹ Armando Somintac,¹ Elmer Estacio,¹ Christopher T. Que,² Satoshi Tsuzuki,³ Kohji Yamamoto,³ and Masahiko Tani³

¹National Institute of Physics, University of the Philippines, Diliman, Quezon City 1101 Philippines

²Department of Physics, De La Salle University, Manila 2401 Philippines

³Research Center for Development of Far-Infrared Region, University of Fukui, Fukui 910-8507, Japan

(Received 26 October 2012; accepted 28 January 2013; published online 11 February 2013)

Terahertz (THz) emission from GaAs-AlGaAs core-shell nanowires (CSNW) on silicon (100) substrates was investigated using THz time-domain spectroscopy. The applied magnetic field polarity dependence strongly suggests that THz emission originated from photo-carriers in the CSNWs. Optical excitation of the GaAs-AlGaAs core-shell yielded a wider THz emission bandwidth compared with that of just the GaAs core material. This result is currently attributed to faster carrier lifetimes in the AlGaAs shell. The THz emission spectral data are supported by time-resolved photoluminescence studies. © 2013 American Institute of Physics. [http://dx.doi.org/10.1063/1.4791570]

Semiconductor nanowire (NW) growth and characterization continue to be the subject of fundamental and applied research. A number of growth techniques, doping methods, and heterostructure designs have been developed to attain desired crystallinity, uniformity, and electro-optic properties of these nanostructures.^{1–4} One such example is the core-shell NW (CSNW) design where the low band gap NW core is coated by a higher band gap shell. This results in the separation of the carriers in the core from the surface traps which enhances the recombination and transport of photo-generated carriers.^{5–7} Similarly, a number of characterization methods have been employed to evaluate NW morphology, crystal structure, and carrier behavior.^{8–11} Rather recently, optical-pump terahertz (THz)-probe measurements have been employed to survey carrier recombination and transport in NWs.^{7,12} However, these earlier reports have not been able to distinguish between the THz characteristics of the core and the shell layers. At present, even as THz emission has been demonstrated for NWs,^{13–15} that of GaAs-AlGaAs CSNWs has not been widely investigated.

In this paper, we investigate the THz emission of GaAs-AlGaAs CSNWs using THz time domain spectroscopy (THz-TDS). Magnetic field polarity dependence strongly suggests that the THz emission originates from the CSNWs and not from the two dimensional (2D) amorphous film on the substrate surface. Selective excitation of the GaAs core or the GaAs-AlGaAs core-shell allowed for the independent qualitative investigation of the core and shell carrier dynamics.

The CSNWs were grown on Si (100) substrates using molecular beam epitaxy via vapor-liquid-solid growth mechanism using Au nanoparticles as catalysts. A SEM micrograph of a CSNW sample is shown in Fig. 1(a). The CSNWs have diameters of 100–150 nm, lengths of 3–8 μm , and a density of $1.60 \times 10^8 \text{ cm}^{-2}$. The CSNW structure consists of a GaAs core, an AlGaAs shell, and a Si-doped GaAs skin having respective nominal growth equivalent film thicknesses of 0.65 μm , 0.84 μm , and 0.1 μm . It must be noted that these

nominal growth equivalent film thicknesses would result in the formation of CSNWs with diameters of 100–150 nm, due to the Au nanoparticles, and a 2D amorphous film on the substrate surface. The thickness of the AlGaAs shell was estimated to be 50–60 nm by comparing the diameters of CSNWs and uncoated GaAs NWs grown using the same growth parameters. The thickness of the n-GaAs skin was considered thin enough to have minimal contribution to the THz emission. It can be observed that the CSNWs are oriented at an angle relative to the substrate surface due to preferential growth in the $\langle 111 \rangle$ direction.¹⁶ The room temperature photoluminescence (PL) of the CSNW in this study is shown in Fig. 1(b). In the PL measurement, the excitation source was an Ar⁺ laser with a wavelength of 488 nm. PL peaks close to the corresponding nominal values of the GaAs and AlGaAs room temperature bandgaps were observed at around 800 nm and 870 nm, respectively. The AlGaAs mole fraction was $x \approx 0.10$ which is expected to yield a PL peak close to 800 nm at room temperature.

Standard THz-TDS measurements were performed in the oblique reflection excitation geometry. The excitation source was a mode-locked Ti:sapphire laser emitting 100 fs pulses at a repetition rate of 80 MHz. The THz emission was detected by an optically gated LT-GaAs photoconductive dipole antenna. The THz induced transient photocurrent was fed to a lock-in amplifier using the 2 kHz mechanically chopped excitation laser as reference. To study the effects of the applied 650 mT magnetic field parallel to the substrate surface, the field polarity was switched between B_{up} and B_{down} and compared with the THz emission with the no-field case (No B). The selective excitation of the GaAs core-only or the GaAs-AlGaAs core-shell was achieved by tuning the excitation wavelength to 850 nm or 775 nm, respectively.

The time domain data and the corresponding Fourier transform spectra of the GaAs-AlGaAs CSNWs for B_{up} , B_{down} and No B cases are shown in Figs. 2(a) and 2(b). Similar measurements for semi-insulating (SI) GaAs substrates are also shown for comparison in Figs. 2(c) and 2(d). The THz emission from the SI-GaAs increased in intensity regardless

^{a)}E-mail: jibanez@nip.upd.edu.ph.

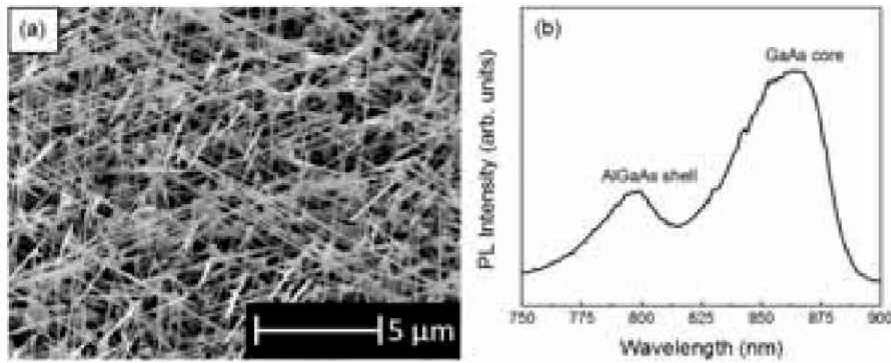


FIG. 1. (a) SEM micrograph of GaAs-AlGaAs CSNWs deposited on Si (100) substrates. The CSNWs are tilted relative to substrate surface. (b) Room temperature photoluminescence spectra of the GaAs-AlGaAs CSNWs showing the peaks associated with the GaAs core and AlGaAs shell.

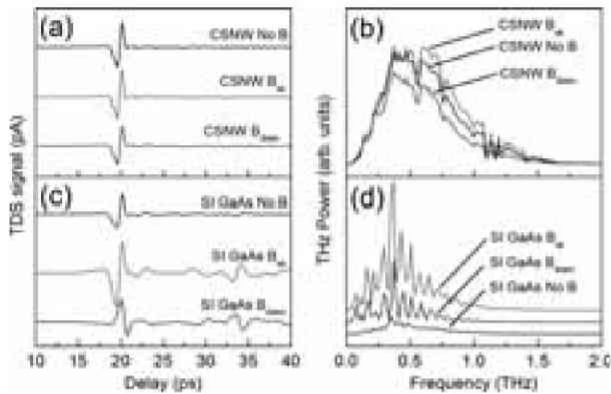


FIG. 2. TDS signal and THz power spectra from (a) and (b) the GaAs-AlGaAs CSNWs and (c) and (d) the Si-GaAs substrate without a magnetic field (No B), with a B_{up} polarity and with a B_{down} polarity. The THz power spectra of the Si-GaAs substrate were vertically offset for ease of comparison.

of the polarity of the applied magnetic field relative to the No B case. On the other hand, for GaAs-AlGaAs CSNW, although an increase in the THz emission intensity was observed for the B_{up} polarity, the intensity decreased for the B_{down} polarity; even less than the No B case.

The enhancement of THz emission by the application of a magnetic field on a bulk THz emitter has been observed and explained in a number of previous works.^{17–20} The anomalous magnetic field enhancement observed in this work is explained in Fig. 3. In bulk semiconductors, photo-generated

carriers move perpendicular to the surface. As a result, the dipole moment of the THz emission is also oriented perpendicular to the surface in the absence of a magnetic field as shown in Fig. 3(a). Under magnetic field, the dipole axis becomes tilted relative to the substrate surface according to the Lorentz force as shown in Figs. 3(b) and 3(c).¹⁷ However, for the CSNWs, carrier movement occurs along the CSNW's axis. Consequently, the dipole moment is also oriented along the same axis. In the case of a CSNW structure tilted relative to surface, as shown in Fig. 3(d), the dipole moment should similarly be tilted even in the absence of an applied magnetic field. If a magnetic field is then applied, the dipole moment is reoriented, as shown in Figs. 3(e) and 3(f), which result to either an increase or decrease in the detected THz emission depending on the field polarity. In fact, the CSNW B_{down} case, in Fig. 3(f), resembles the dipole moment orientation of the bulk sample for the No B case. This peculiar magnetic field polarity dependence of the THz emission strongly suggests that THz emission originates from the transient current along the NW axis and not from the 2D amorphous film on the substrate surface.

The CSNW THz emission spectra for the selective excitation of the GaAs-AlGaAs core-shell (775 nm) and the GaAs core-only (850 nm) are shown in Fig. 4(a). The THz emission from the excitation of the GaAs-AlGaAs core-shell has a wider spectrum than that from the excitation of just the core material. The higher-frequency components suggest that carriers from the AlGaAs shell material are characterized by faster carrier lifetimes (as compared to carriers from the GaAs

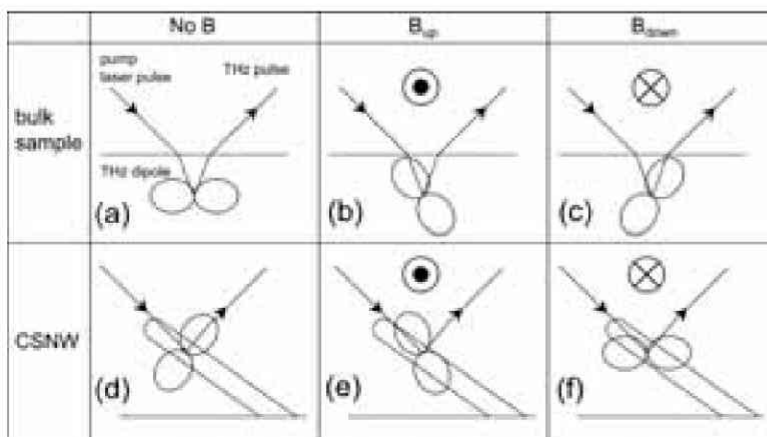


FIG. 3. The THz emission dipole from a planar semiconductor (a)–(c) and a CSNW (d)–(f) with and without an applied magnetic field. The dipole orientation is similar for (a) and (f); (b) and (e); and (c) and (d).

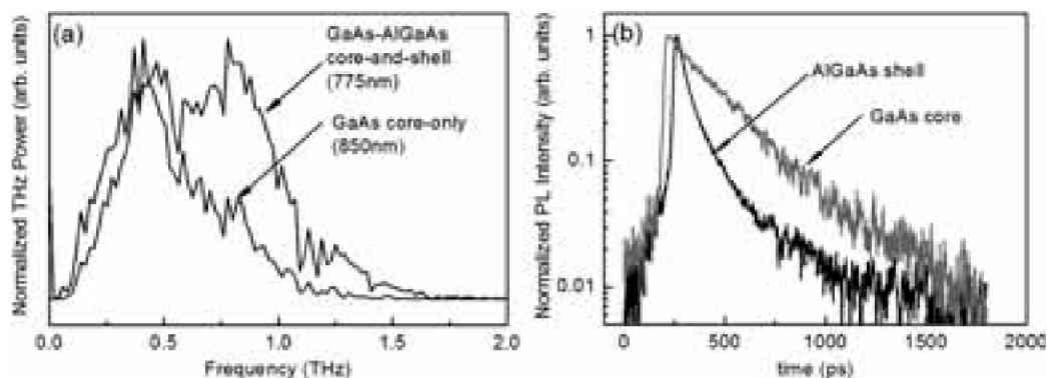


FIG. 4. (a) THz emission from the selective excitation of the GaAs-AlGaAs core-shell and of only the GaAs core. The excitation wavelengths are 775 nm for the GaAs-AlGaAs core-shell and 850 nm for only the GaAs core. (b) Time resolved PL of the GaAs core and AlGaAs shell. The PL intensity of the AlGaAs decays faster than that of the GaAs.

core). Upon ultrafast optical excitation, photo-generated carriers undergo drift transport along the nanowire axis before slowing down and eventually recombining, radiatively. In a ballistic transport picture, higher velocity carriers contribute to higher-frequency THz emission while slower carriers correspond to lower frequencies. As such, short carrier lifetimes should yield higher-frequency THz emission. The longer lifetime carriers are expected to slow down thereby producing lower frequency THz components. This result is supported by the time-resolved PL (TRPL) spectra of the CSNWs, shown in Fig. 4(b); where the carrier recombination lifetime in the AlGaAs shell is faster than that of the GaAs core. This experimental demonstration of the independent qualitative study of the carrier dynamics of the core and shell materials using THz emission spectroscopy may prove vital in further improvements of GaAs-AlGaAs CSNW growth designs.

An anomalous magnetic field polarity dependence of the THz emission intensity for CSNWs was observed. This is attributed to the THz emission originating from photo-carrier drift along the CSNW axis. Optical excitation of the GaAs-AlGaAs core-shell reveal wider frequency THz emission, compared with the excitation of just the GaAs core. This bandwidth difference is related to the faster carrier lifetimes in the AlGaAs shell compared to the GaAs core material. The THz emission spectroscopy data are supported by TRPL measurements.

This work was undertaken with grants from the University of the Philippines (UP) Systems Grant, UP Office of the Vice-Chancellor for Research and Development, and the Department of Science and Technology.

¹J. Noborisaka, J. Motohisa, S. Hara, and T. Fukui, Appl. Phys. Lett. **87**, 093109 (2005).

- ²D. Spirkoska, J. Arbiol, A. Gustafsson, S. Conesa-Boj, F. Glas, I. Zardo, M. Heigoldt, M. H. Gass, A. L. Bleloch, S. Estrade, M. Kaniber, J. Rossler, F. Peiro, J. R. Morante, G. Abstreiter, L. Samuelson, and A. Fontcuberta i Morral, Phys. Rev. B **80**, 245325 (2009).
- ³C. Colombo, M. Heiß, M. Graetzel, and A. Fontcuberta i Morral, Appl. Phys. Lett. **94**, 173108 (2009).
- ⁴D. Lucot, F. Jabeen, J.-C. Harmand, G. Patriarche, R. Giraud, G. Faini, and D. Mailly, Appl. Phys. Lett. **98**, 142114 (2011).
- ⁵P. Prete, F. Marzo, P. Paiano, N. Lovergine, G. Salviati, L. Lazzarini, and T. Sekiguchi, J. Cryst. Growth **310**, 5114–5118 (2008).
- ⁶F. Jabeen, S. Rubini, V. Grillo, L. Felisari, and F. Martelli, Appl. Phys. Lett. **93**, 083117 (2008).
- ⁷P. Parkinson, H. J. Joyce, Q. Gao, H. Hoe Tan, X. Zhang, J. Zou, C. Jagadish, L. M. Herz, and M. B. Johnston, Nano Lett. **9**(9), 3349–3353 (2009).
- ⁸Z. Gu, P. Prete, N. Lovergine, and B. Nabet, J. Appl. Phys. **109**, 064314 (2011).
- ⁹S. Perera, M. A. Fickenscher, H. E. Jackson, L. M. Smith, J. M. Yarrison-Rice, H. J. Joyce, Q. Gao, H. H. Tan, C. Jagadish, X. Zhang, and J. Zou, Appl. Phys. Lett. **93**, 053110 (2008).
- ¹⁰P. Parkinson, J. Lloyd-Hughes, Q. Gao, H. Hoe Tan, C. Jagadish, M. B. Johnston, and L. M. Herz, Nano Lett. **7**(7), 2162–2165 (2007).
- ¹¹L. Yang, J. Motohisa, T. Fukui, L. Xi Jia, L. Zhang, M. M. Geng, P. Chen, and Y. Liang Liu, Opt. Express **17**(11), 9337–9346 (2009).
- ¹²J. H. Strait, P. A. George, M. Levendorf, M. Blood-Forsythe, F. Rana, and J. Park, Nano Lett. **9**(8), 2967–2972 (2009).
- ¹³G. B. Jung, Y. J. Cho, Y. Myung, H. S. Kim, Y. S. Seo, J. Park, and C. Kang, Opt. Express **18**(16), 16353–16359 (2010).
- ¹⁴D. V. Seletskiy, M. P. Hasselbeck, J. G. Cederberg, A. Katzenmeyer, M. E. Toimil-Molares, F. Léonard, A. Alec Talin, and M. Sheik-Bahae, Phys. Rev. B **84**, 115421 (2011).
- ¹⁵K. J. Kong, C. S. Jung, G. B. Jung, Y. J. Cho, H. S. Kim, J. Park, N. E. Yu, and C. Kang, Nanotechnology **21**, 435703 (2010).
- ¹⁶K. Hiruma, M. Yazawa, T. Katsuyama, K. Ogawa, K. Haraguchi, M. Koguchi, and H. Kakibayashi, J. Appl. Phys. **77**(2), 447 (1995).
- ¹⁷M. B. Johnston, D. M. Whittaker, A. Corchia, A. G. Davies, and E. H. Linfield, Phys. Rev. B **65**, 165301 (2002).
- ¹⁸M. B. Johnston, D. M. Whittaker, A. Corchia, A. G. Davies, and E. H. Linfield, J. Appl. Phys. **91**(4), 2104–2106 (2002).
- ¹⁹C. Weiss, R. Wallenstein, and R. Beigang, Appl. Phys. Lett. **77**(25), 4160–4162 (2000).
- ²⁰N. Sarukura, H. Ohtake, S. Izumida, and Z. Liu, J. Appl. Phys. **84**, 654 (1998).